

VEHICLE DYNAMICS MODEL AS ROAD PAVEMENT LOAD GENERATOR

Z. L O Z I A

WARSAW UNIVERSITY OF TECHNOLOGY, FACULTY OF TRANSPORT

75 Koszykowa St., 00-662 Warsaw, POLAND

e-mail: lozia@it.pw.edu.pl

This paper presents the models of vehicle that are treated as road pavement load generators for different motion cases. The key role of a tire model is discussed. The most complicated 14 degrees of freedom truck model is based on the structure of a biaxial vehicle with dependently suspended front and rear wheels. The road pavement is treated as rigid but uneven. The road irregularities have a determined 3D form and may also be the realisation of stationary Gaussian random process describing the real road according to ISO recommendations. The paper shows specific model application for generation of forces between tires and uneven road. The vehicle response (for given motion cases, e.g. straight constant velocity motion) may be presented as time histories of footprint forces as well as force's PSD. The simulation results may be treated as input data for the road pavement stress and wear analysis.

Key Words: wheel/pavement force, vehicle dynamics model.

1. INTRODUCTION

The author's main area of interest is vehicle motion and dynamics simulation as well as their analysis. However, the models used for this purpose are also useful in road pavement load description. When examining the vehicle model, a very strong initial assumption has been made: the road surface is uneven but undeformable. This assumption may be acceptable because of the difference between the tire and pavement stiffness coefficients.

The paper presents a set of vehicle models that may be treated as road pavement load generators. The key element of the vehicle model is the model of tire radial properties.

2. VEHICLE MODELS

Figure 1 presents the simplest vehicle model: a *quarter-car model* with two degrees of freedom. It has two masses, a sprung mass m_A and an unsprung mass m_P . They are moving vertically. Vertical displacements z_A and z_P are the two degrees of freedom. The suspension spring force as well as the damping force are generally non-linear, including suspension limiters, dry friction and the asymmetry of shock absorber characteristics. q_P represents the road profile height for the current model position $x_A = x_P$. The tire model is one of the six models presented below.

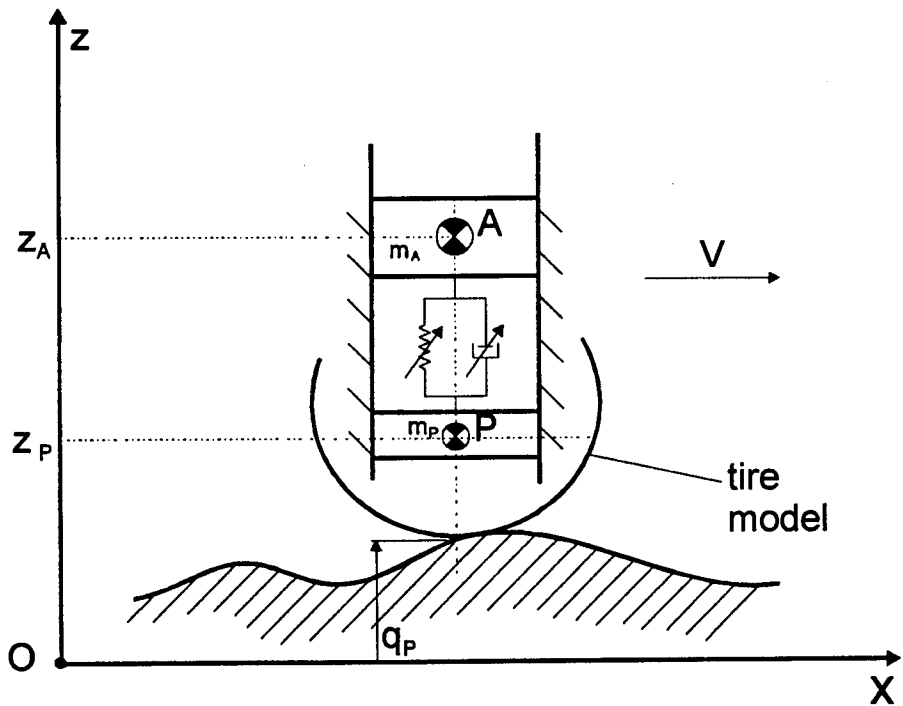


FIG. 1. Quarter-car model.

Figure 2 shows a biaxial two-dimensional vehicle model. When considering the suspension unsprung mass and tire, it is the same as the *quarter-car* as regards the front and rear axle. Sprung mass is represented by a rigid beam, which has mass m and pitch moment of inertia I_M . q_P and q_T are road profile heights, for front and rear axle, respectively. The model has four degrees of freedom: sprung mass vertical displacement z_M and pitch angle φ_M , two unsprung masses vertical displacements z_P, z_T .

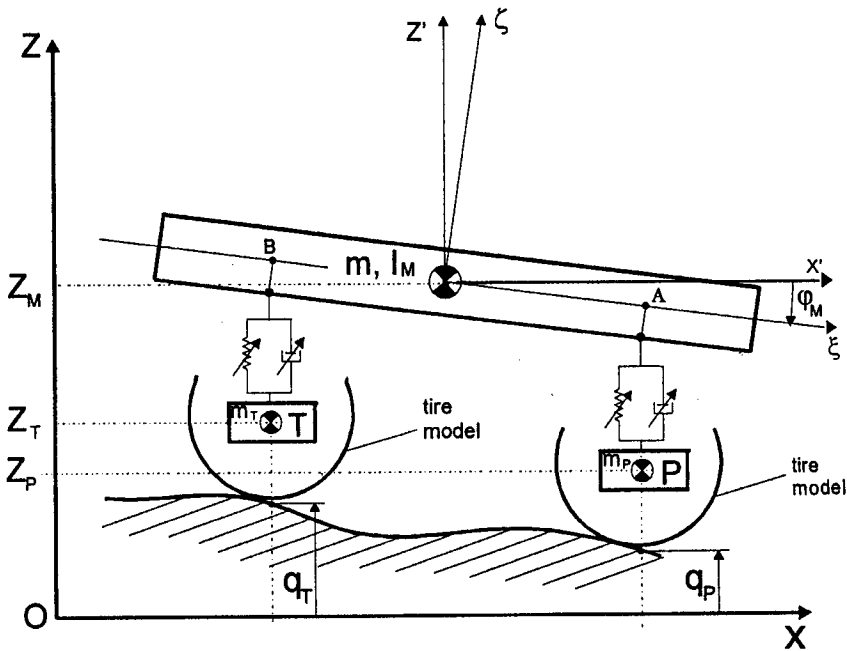


FIG. 2. Biaxial two-dimensional vehicle model.

For both models presented in Figs. 1 and 2 constant straight-line velocity is assumed.

Figure 3 shows a three-dimensional truck model based on the structure of a biaxial vehicle with dependently suspended front and rear wheels. It consists of seven rigid mass elements: body, front and rear axle beam, four rotating wheels. The vehicle motion is described in an immovable system $Oxyz$ connected with the road and in many local systems connected with model bodies. The model has 14 degrees of freedom: 3 co-ordinates of vehicle body centre of gravity O_1 position in fixed system $Oxyz(x_{01}, y_{01}, z_{01})$, 3 angular co-ordinates of body position (yaw ψ_1 , pitch φ_1 and roll ϑ_1), 4 co-ordinates of unsprung masses relative motion (ζ_{104} , ϑ_4 , ζ_{109} , ϑ_9), 4 angular co-ordinates of wheels' rotation (φ_5 , φ_6 , φ_7 , φ_8).

Non-linear elastic-damping suspension characteristics were adopted, including nonlinearities (limiters, dry friction, asymmetry of shock absorbers). The pneumatic tire model (see LOZIA [11] and LOZIA [15]) describes interaction with even and uneven road surface. Account has been taken of elastic and damping properties in the radial direction and of elastic properties in the lateral and longitudinal directions. The tire share forces and the aligning moment model is a semi-empirical model (HSRI-UMTRI, see FANCHER *et al.* [5], or MAGIC FORMULA, see PACEJKA [16]). Account has also been taken of the influence of kingpin inclination, caster, and toe-in angles on forces and moments generated

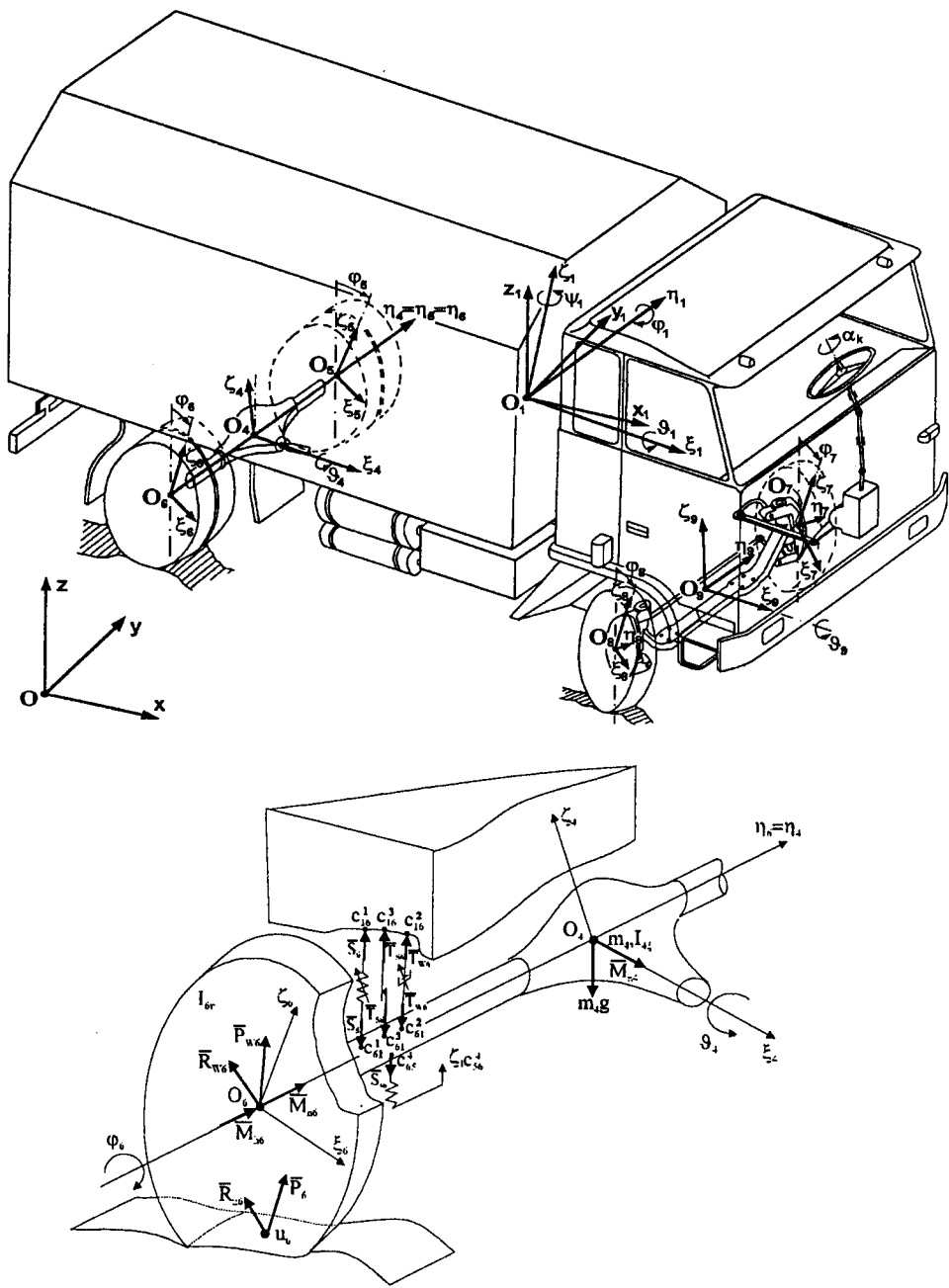


FIG. 3. Biaxial truck model structure together with assumed coordinate systems. Suspension and tire-road contact forces and moments.

in the footprint. The shortest wavelength of road profile is about $3 \div 5$ times longer than the average footprint length. The road surface irregularities have a determined 3D form. The steering system model, apart from geometric properties, describes also its elastic properties. Force and moment inputs result from the aerodynamic drag, wheel rolling resistance, braking, driving. The steering wheel angle is treated as external input. Experimental verifications have been performed (see LOZIA, STEGIENKA [13], LOZIA [14]) on an even road surface for the manoeuvres recommended by ISO [6 – 8]: the steady state circular test, the step input test and the severe lane-change manoeuvre. Good compatibility between simulation and experiment has been obtained.

3. TIRE RADIAL PROPERTIES MODELS

Figure 4 presents six tire radial properties models: *point contact*, *rigid tread band*, *fixed footprint*, *variable footprint length*, *radial spring*, *adaptive footprint*.

The *point contact tire model (PCTM)* is represented by a parallel nonlinear spring-dashpot combination that interacts with the road profile through a point follower. The simplest version of the model assumes linear characteristics of spring and dashpot and a lack of wheel hops. PCTM is the most popular tire radial model.

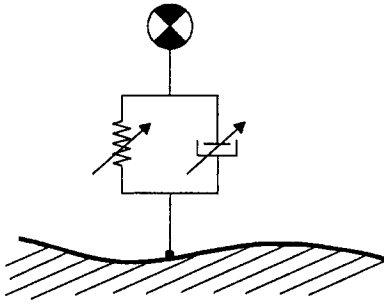
The *rigid tread band tire model (RTBTM)* is similar to PCTM but it interacts with the road profile through a roller follower of radius equal to the tire radius (see CAPTAIN *et al.* [2]).

The *fixed footprint tire model (FFTM)* interacts with the road through a footprint of a constant length. When assuming linear characteristics of elementary spring-dashpot element, it is possible to replace FFTM with PCTM by averaging the road profile elevation taken across the footprint length (see CAPTAIN *et al.* [2]).

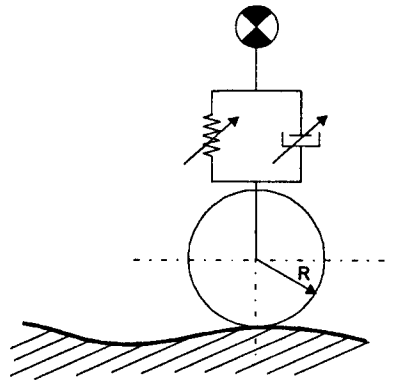
The *variable footprint length tire model (VFLTM)* is similar to FFTM but the footprint length is not constant. It depends on the previous simulation step resultant tire vertical force (see LOZIA [11]).

The *radial spring tire model (RSTM)* consists of springs spanning radially outward from the wheel centre (see DAVIS [4]). BERNARD *et al.* [1] has modified the RSTM model by limiting the relative deflection of neighbouring radial springs.

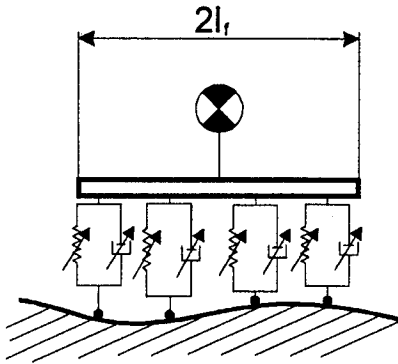
The *adaptive footprint tire model (AFTM)* consists of flexible tread band inflated by internal pressure and linked to the wheel centre by angularly distributed stiffness and damping that simulate the carcass and tread stiffness (see CAPTAIN *et al.* [2]). LOZIA [12] has modified the AFTM. Tangential properties of a tire were added as well as BERNARD'S [1] limitation of radial deflection of the discretized AFTM model.



Point contact tire model (*PCTM*)

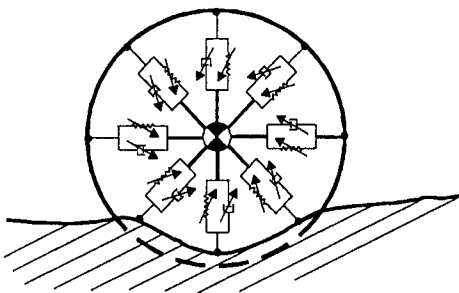


Rigid tread band tire model (*RTBTM*)

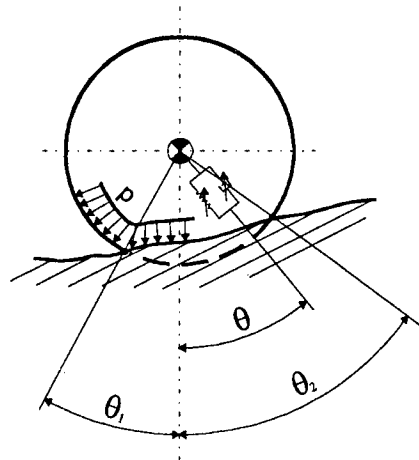


Fixed footprint tire model (*FFTM*)
 $2l_f = \text{const}$

Variable length footprint tire model (*VFLTM*)
 $2l_f = \text{variable}$



Radial spring tire model (*RSTM*)



Adaptive footprint tire model (*AFTM*)

FIG. 4. Six models of tire radial properties.

All the listed models may be used in the *quarter-car* vehicle model as well as in the biaxial two-dimensional vehicle model. The three-dimensional vehicle model accepts only *the point contact and the fixed footprint tire model*.

4. ROAD PROFILE

For two simple vehicle models (Figs. 1 and 2), the road surface irregularities are described in space co-ordinate x or in frequency (wave number) domain using the power spectral density (PSD). For the complex vehicle model (Fig. 3), the road surface irregularities have a determined 3D form and may also be the realisation of a stationary Gaussian random process describing real road according to the ISO recommendations [9]. The road of a given class is described by vertical irregularities PSD of the longitudinal track and coherence function of parallel tracks. Figure 5 presents an exemplary realisation of the road profile.

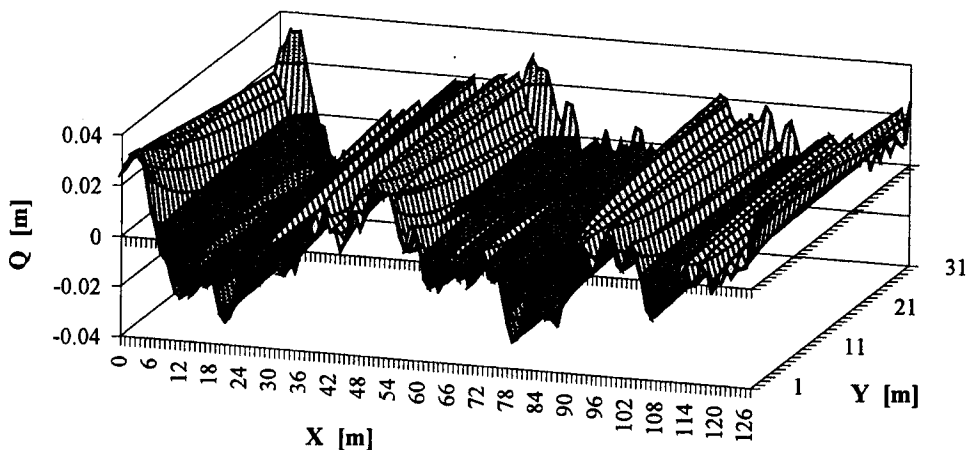


FIG. 5. Exemplary realisation of 3D road surface irregularities, generated on the basis of ISO recommendations. Average road (D class), standard deviation $\sigma = 0.01429$ mm. Basefull rectangle: 127×31 m. Net step: $1\text{m} \times 1\text{m}$.

5. COMPARISON OF TIRE RADIAL PROPERTIES MODELS

A wide comparison has been done in works of CAPTAIN *et al.* [2], BERNARD *et al.* [1], LOZIA [11], KISIŁOWSKI and LOZIA [10].

Two models can be transformed into *the point contact tire model* by using the road profile smoothing. For *the fixed footprint model* it is possible to derive the tire filter transfer function analytically (see Fig. 6, $f_L = 1/L$ is the wave number,

L means wavelength, l_f is half of the footprint static length). For the rigid tread band model, the smoothing process is a step-by-step solution to the problem of possible contact between the rigid wheel and uneven profile. Figure 7 presents original and smoothed road profiles for the rigid tread band model. This kind of smoothing may be called "geometrical smoothing".

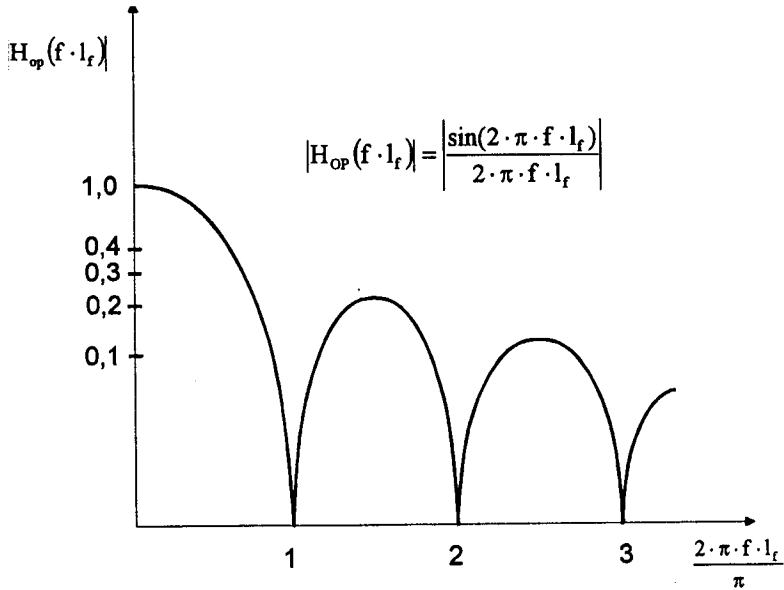


FIG. 6. Modulus of tire transfer function for fixed footprint model.

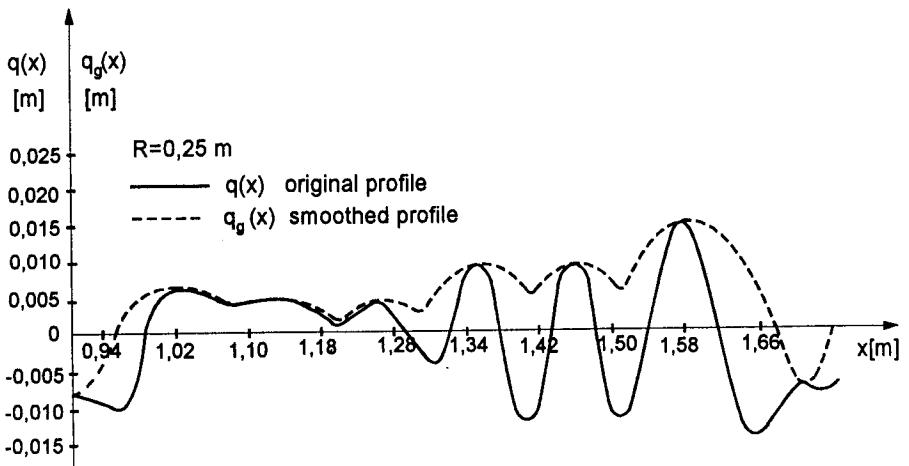


FIG. 7. "Geometrical smoothing" by rigid tread band tire model.

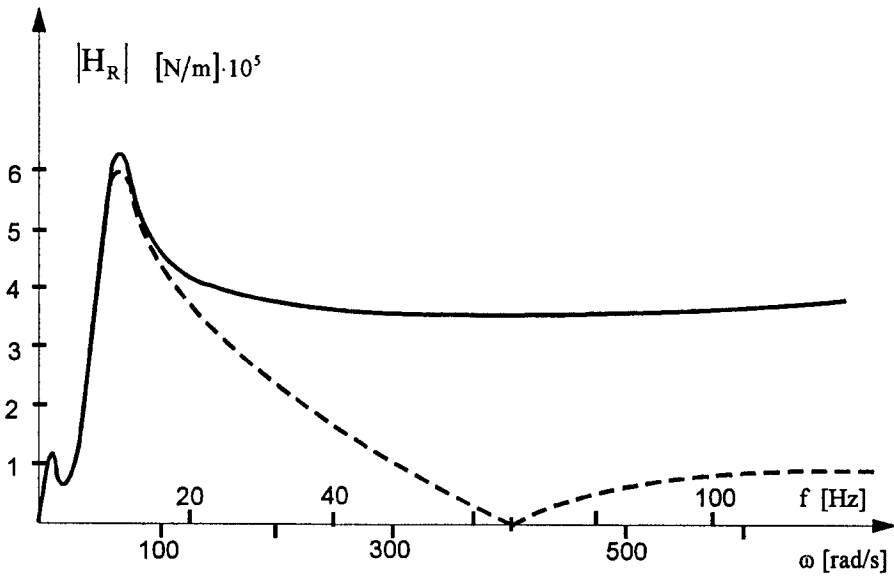


FIG. 8. Modulus of transfer function of rear tire vertical dynamic force. Middle class car. Two tire models: — point contact, - - - - fixed footprint.

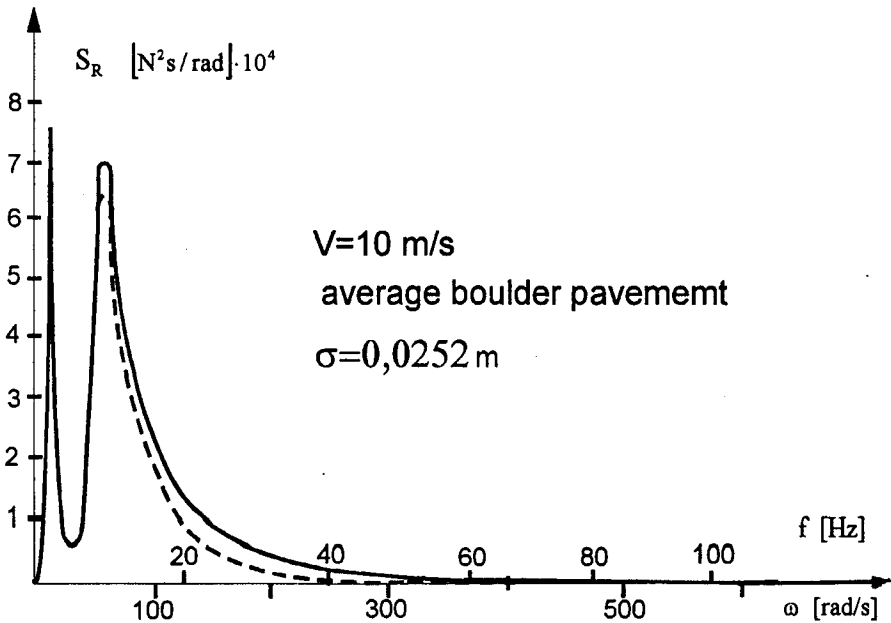
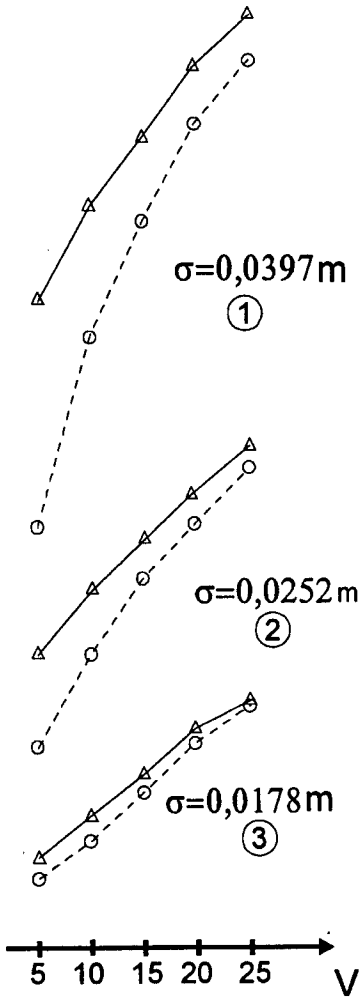


FIG. 9. Power spectral density (PSD) of rear tire vertical dynamic force. Average boulder pavement. Middle class car. Two tire models: — point contact, - - - - fixed footprint.

σ_{FP} - front wheel



σ_{FT} - rear wheel

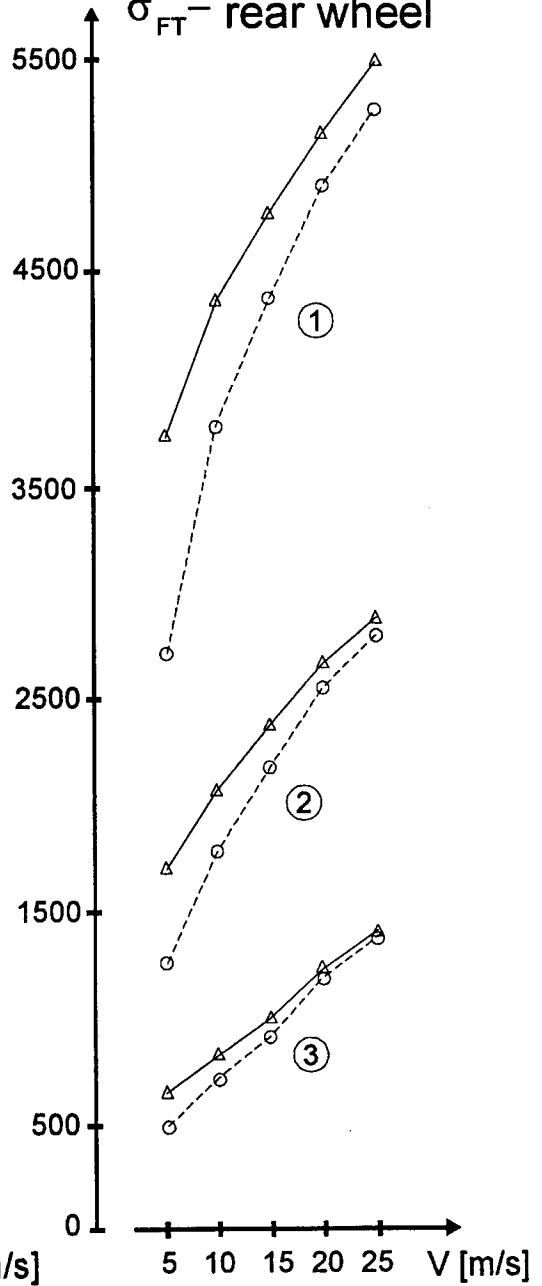


FIG. 10. Standard deviation of the footprint vertical dynamic tire force as a function of vehicle velocity. Middle class car. Three types of road irregularities: 1 - very poor boulder pavement, 2 - average boulder pavement, 3 - poor asphalt-concrete. Two tire models: — point contact, - - - - fixed footprint.

Short wavelength smoothing plays an important role. The following examples will describe it. When applying a linear biaxial two-dimensional vehicle model (Fig. 2 but with linearised properties of suspension and tires), it is possible to derive the transfer function of footprint vertical forces (front and rear). Figure 8 presents a comparison of the above mentioned transfer function for rear wheels of a medium class car ($l_f = 0.078$ m) when applying *the point contact tire model* and *the fixed footprint tire model*. Figure 9 shows PSD of the tire vertical dynamic force for both tire models. For frequency higher than 10 Hz the role of smoothing properties of a tire is very important. Figure 10 presents a comparison of standard deviations of middle class car footprint vertical dynamic forces. They are shown as functions of the vehicle velocity. Results are given for the front and rear wheels, for three types of road: asphalt-concrete in a bad condition, an average boulder pavement and a very poor boulder pavement. σ denotes standard deviation of the road profile. The role of tire smoothing is higher for lower velocities and for worse roads.

6. EXEMPLARY RESULTS OF CALCULATIONS FOR A 12-TON TRUCK

Exemplary results of calculation for a 12-ton truck and road pavement in an average condition (see ISO [9]) are presented below. Main attention is paid to the role of suspension damping properties. Table 1 presents seven combinations of vehicle parameters: from vehicle #1 (nominal hydraulic damping in shock absorbers and nominal dry friction in suspension elements) to a rather theoretical case of vehicle #7 (without any damping in suspension).

Table 1. Seven different vehicle's suspension damping combinations

| Vehicle code | Level of hydraulic damping in shock absorbers [%] | Level of dry friction in suspension [%] |
|--------------|---|---|
| #1 | 100 | 100 |
| #2 | 50 | 100 |
| #3 | 0 | 100 |
| #4 | 50 | 50 |
| #5 | 100 | 0 |
| #6 | 50 | 0 |
| #7 | 0 | 0 |

The nominal vehicle is characterized by the following level of relative suspension dry friction (relation between static dry friction force and static wheel load on even, horizontal road):

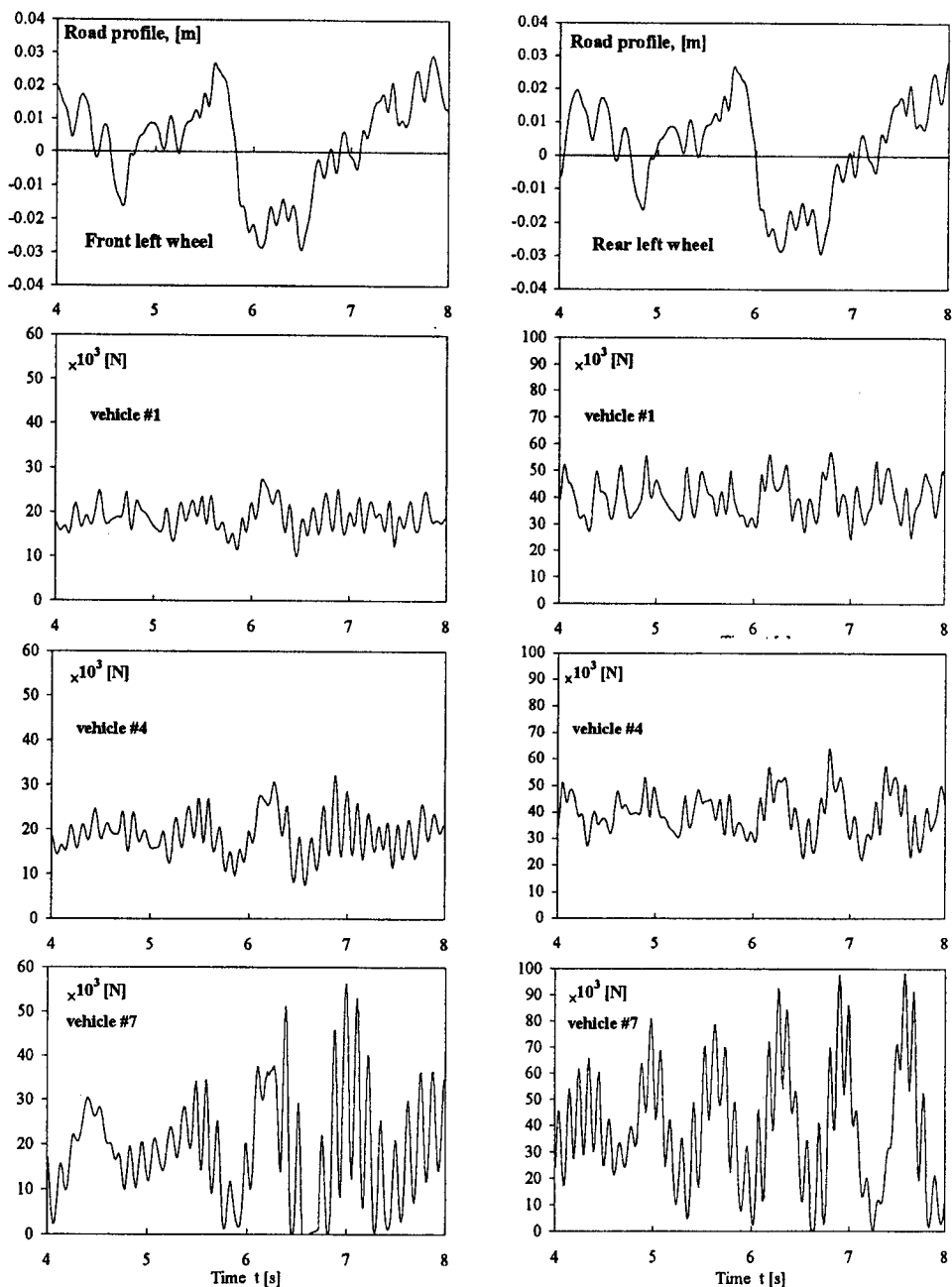
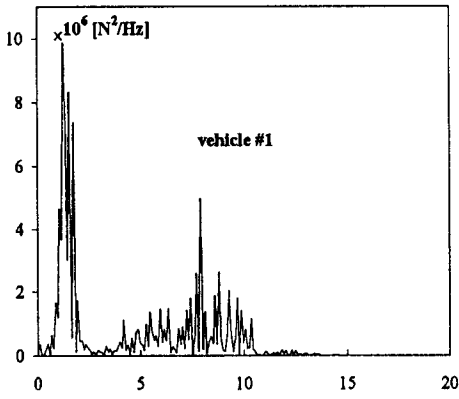


FIG. 11. Exemplary time histories of vertical component of the footprint force together with road profile height. Road pavement in average condition. $V = 80$ km/h. Left column: front left wheel. Right column: rear left wheel.

Front left wheel



Rear left wheel

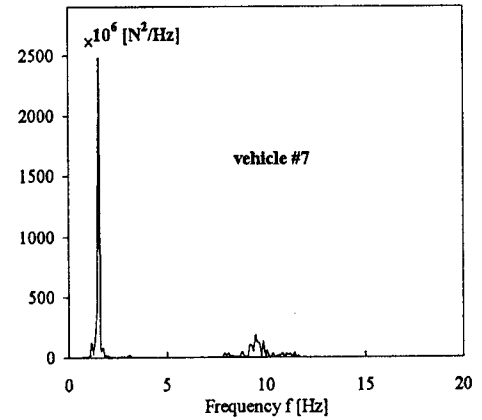
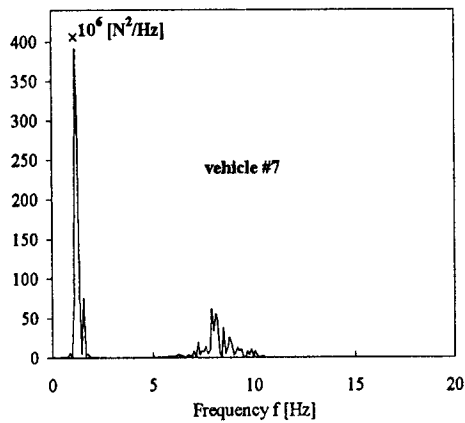
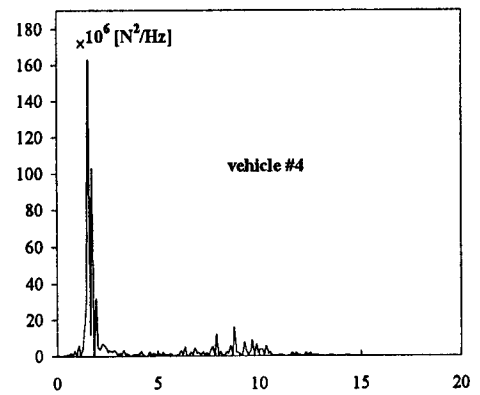
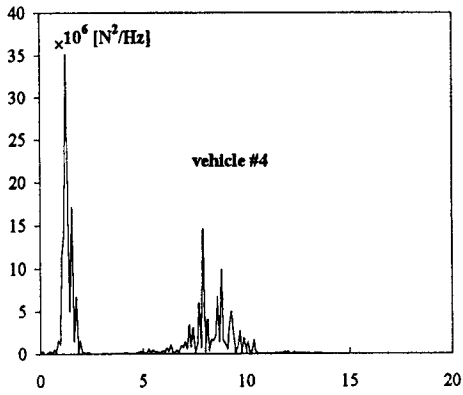
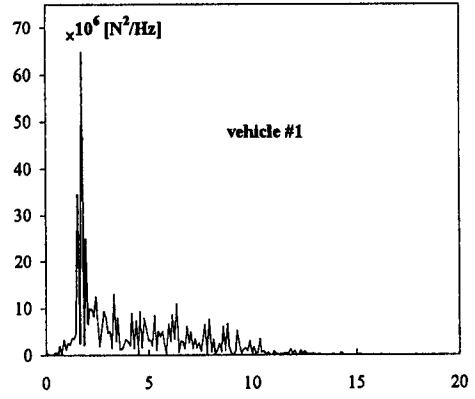


FIG. 12. Power spectral density (PSD) of vertical component of the footprint force. Road pavement in average condition, $V = 80$ km/h. Left column: front left wheel. Right column: rear left wheel.

- 3.9% for front wheels,
- 13.9% for rear wheels.

This shows that relative dry friction is more than 3 times higher for rear wheel's suspension.

General influence of damping may be observed by comparing the results for vehicles: #1, #4, #7. The influence of hydraulic damping in shock absorbers is observed when comparing vehicles: #1, #2, #3 or #5, #6, #7. The role of dry friction is visible by comparing the results obtained for vehicles #2, #4 and #6.

Figure 11 presents comparison of 4 second time histories of vertical component of the front left and rear left footprint force for vehicles: #1, #4 and #7, as well as the road profile height in the middle of the tire-road contact area. The lower is the suspension damping, the larger will be the oscillations of vertical footprint force. For the theoretical case (vehicle #7 without suspension damping) a wheel hop occurs.

Figure 12 shows PSDs obtained for 10.24 sec. (0.01 sec. time step, 0.22 m distance step) of time histories of footprint vertical forces shown in Fig. 11. The lower is the suspension damping, the larger will be the role of oscillations from the range of $1 \div 3$ Hz and $7 \div 11$ Hz (which are the 1st and 2nd natural frequency of linearised vehicle model).

Figure 13 presents the results for vehicles #1, #4 and #7 in the form of relationship between:

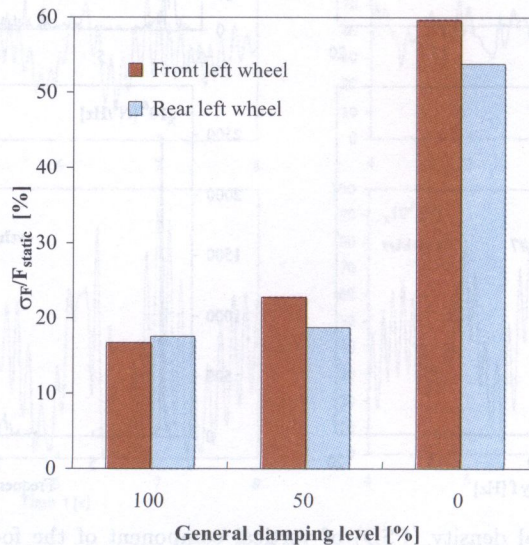


FIG. 13. Vertical footprint force standard deviation σ_F related to the vertical footprint static force F_{static} as a function of general suspension damping level: 100% - vehicle #1; 50% - vehicle #4; 0% - vehicle #7.

- the vertical footprint force standard deviation σ_F related to the vertical footprint static force (expressed in %), and
- the general suspension damping level (both hydraulic damping of shock absorbers and dry friction level, expressed in % of the nominal state for vehicle #1).

Figure 14 contains similar results for vehicles #2, #4, #6 showing the influence of the dry friction level. Figures 15 and 16 present the influence of hydraulic damping level for nominal dry friction (Fig. 15, vehicles: #1, #2, #3) and for the theoretical case when there is no dry friction in suspension (Fig. 16, vehicles: #5, #6, #7).

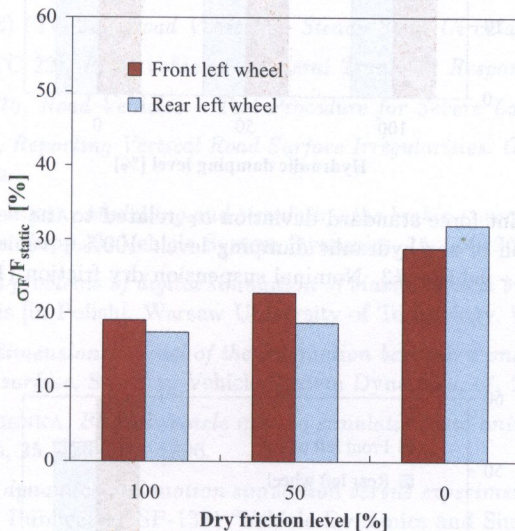


FIG. 14. Vertical footprint force standard deviation σ_F related to the vertical footprint static force F_{static} as a function of the suspension dry friction level: 100% - vehicle #2; 50% - vehicle #4; 0% - vehicle #6. Hydraulic damping level: 50%.

The lower is the damping, the higher will be the oscillations of the footprint vertical force (see also Figs. 11 and 12). The role of hydraulic damping in shock absorbers is more significant for lower dry friction level (Figs. 15 and 16 for front wheel).

High suspension dry friction should be avoided because of worse static load sharing between the left and right wheel, unpredictable static position of suspension and higher wear of suspension elements. That shows the important role of hydraulic shock absorbers in heavy vehicles.

The results presented above can be treated as input data for the road pavement stress and wear analysis. Exemplary results of such attempts are published, e.g. in the paper by CEBON [3].

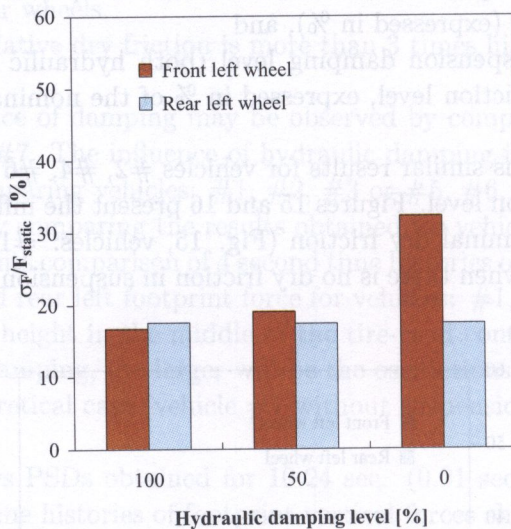


FIG. 15. Vertical footprint force standard deviation σ_F related to the vertical footprint static force F_{static} as a function of the hydraulic damping level: 100% - vehicle #1; 50% - vehicle #2; 0% - vehicle #3. Nominal suspension dry friction (100%).

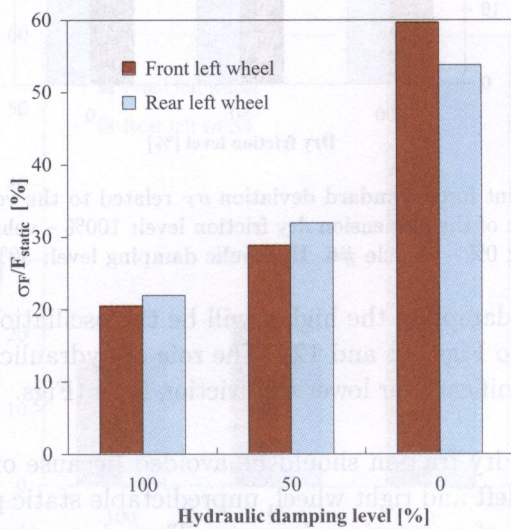


FIG. 16. Vertical footprint force standard deviation σ_F related to the vertical footprint static force F_{static} as a function of the hydraulic damping level: 100% - vehicle #5; 50% - vehicle #6; 0% - vehicle #7. Lack of suspension dry friction (0%).

REFERENCES

1. J. BERNARD, M. VANDERPLOEG, R. JANE, *Tire Models for Determination of Vehicle Loads*, Proceedings of 7th IAVSD Symposium, Cambridge UK, 141–153, September, 1981.
2. K. M. CAPTAIN, A. B. BOGHANI, D. N. WORMLEY, *Analytical Tire Models for Dynamic Vehicle Simulation*, Vehicle System Dynamics, **8**, 1–32, 1979.
3. D. CEBON, *Interaction Between Heavy Vehicles and Roads*, SAE TP 930001.
4. D. C. DAVIS, *A Radial-Spring Terrain-Enveloping Tire Model*, Vehicle System Dynamics, **4**, 55–69, 1975.
5. P. S. FANCHER Jr., Z. BAREKET, *Including roadway and tread factors in semi-empirical model of truck tyres*, Supp. to Vehicle System Dynamics, **21**, 92–107, 1993.
6. ISO 4138-1982 (E) (TC 22), *Road Vehicles – Steady State Circular Test Procedure*.
7. ISO 7401-1988 (TC 22), *Road Vehicles – Lateral Transient Response Test Method*.
8. ISO/TR 3888/1975, *Road Vehicles – Test Procedure for Severe Lane-Change Manoeuvre*.
9. ISO/TC 108/253, *Reporting Vertical Road Surface Irregularities. Generalised Vertical Road Inputs to Vehicles*.
10. J. KISIŁOWSKI, Z. LOZIA, *Modelling and simulating the braking process of automotive vehicle on uneven surface*, Supp. to Vehicle System Dynamics, **15**, 250–263, 1986.
11. Z. LOZIA, *Selected problems of digital simulation of biaxial vehicle braking process on uneven road*, Ph. D. thesis [in Polish], Warsaw University of Technology, Warsaw 1985.
12. Z. LOZIA, *A two-dimensional model of the interaction between a pneumatic tire and an even and uneven road surface*, Supp. to Vehicle System Dynamics, **17**, 227–238, 1988.
13. Z. LOZIA, I. STEGIENKA, *Biaxial vehicle motion simulation and animation*, Supp. to Vehicle System Dynamics, **25**, 426–437, 1996.
14. Z. LOZIA, *Vehicle dynamics and motion simulation versus experiment*, SAE TP 980220 (also published Special Publication SP-1361 “Vehicle Dynamics and Simulation, 1998”, 1–17, as well as in SAE Transactions, Section 6, **107**, 344–360, 1998).
15. Z. LOZIA, *Model of steered tyred wheel. Three-dimensional problem*, Journal of Theoretical and Applied Mechanics, **35**, 4, 849–870, 1997.
16. H. B. PACEJKA, *The magic formula tyre model*, Supp. to Vehicle System Dynamics, **21**, 1–18, 1993.

Received October 26, 1999.
